MODELING AN OPTICAL DIGITIZER ROBOTIC FOR READING THREE-DIMENSIONAL OBJECTS

Jorge Eliécer Rangel Díaz, jrangel@mecanica.ufu.br
Universidad De La Salle, Facultad de Ingeniería de Diseño y Automatización Electrónica, Bogotá. Colombia
Federal University of Uberlândia, School of Mechanical Engineering, 38400-902 Uberlândia-MG, Brasil

Werley Rocherter Borges Ferreira, wrbferreira@mecanica.ufu.br
Federal University of Uberlândia, School of Mechanical Engineering, 38400-902 Uberlândia-MG, Brasil

João Carlos Mendes Carvalho, jcmendes@mecanica.ufu.br
Federal University of Uberlândia, School of Mechanical Engineering, 38400-902 Uberlândia-MG, Brasil

Abstract. *In several technological and artistic areas it is necessary to obtain the dimensions of three-dimensional objects for its graphical representation and/or reproduction. A general and unique method does not exist to do this task due to the object form, its physical composition and dimensions that make difficult the reading process. To take the object dimensions there are a variety of system, manual or robotics, known as scanners or digitizers, which each of them has its own methods to read dimensions and process then. In this paper is presented the development of a three-dimensional digitizer using a robotic structure with five degrees of freedom. In order to reduce the amount of data, diminish the error sources on the measurements and to reduce the computational costs it was used a methodology, based on the triangulation method, that pursue the normal vector of the three-dimensional surface.*

Keywords*: Digitizers, Optical digitizer, Reverse Engineering, Robotics, Surface digitalization.*

1. INTRODUCTION

It is clear the increasing interest for using computational tools and CAD/CAM softwares to design and produce three dimensional objects. In some cases the physical object exists and must be reproduced. Then its dimensions must be known. Many researches have been made in order to obtain an efficient method to reconstruct three-dimensional surfaces that can be applied to several areas like as medical science, biomedical engineering, geographics data process, paleontology and reverse engineering.

The first step of reconstructing a model is to acquire data of the real object. This can be done by using manual and/or automatic equipment named scanner or digitizer which the output is a collection of points describing the original surface. In the acquisition data process, thousands or millions of data must be acquired due to the resolution and correctness of the final model is highly dependent on the density of distribution of the points. In general the data set is a non-organized cloud of points, with non-uniform sampling density, with gaps and noise. In this way two kinds of equipments have been developed to acquire the surface measures: those whose use measurement techniques with contact and those without contact. Measurements techniques without contact use several physical methods such as optical, magnetic, and others. The techniques with contact in general use a contact sensor to take the surface coordinate when the sensor touches it. The process for reconstruction a real object is known as reverse engineering (Bajaj et al., 1995), (Larsson and Kjellander, 2006), (Moccozet et al., 2004), (Müller et al., 2000), (Remondino, 2003) and (Várady et al., 1997).

Then, a big challenge for a surface reconstruction is to acquire an "ideal" set of points that represents more faith fully to the real object. Thus, the digitizer plays an important role in the reconstruction process. Some difficulties to develop a digitizer are related to dimensions and shape of the object, if the object moves or not, if the surface to be read is inner or out of the object and others. Several digitizers had been developed and examples can be seen in (Feng et al., 2001), (Dalton, 1998), (Milroy et al., 1996), (Larsson and Kjellander, 2006), (Li et al., 2007), (Levoy et al., 1998) and in web sites like as http://graphics.stanford.edu/projects/mich/mgantry-in-lab/mgantry-in-lab.html, http://news.softpedia.com/news/Scan-the-World-43630.shtml, http://www.dpi-3d.com/news/082906 and http://www.cynoprod.com/fileadmin/pdf/CYNOPROD_i3Evolution.pdf.

In this paper it has been described a robotic system to use as digitizer. The system works as a left and right hand where the left hand take the object and the right one manipulates an optical sensor to "read" the surface coordinates. After the system description, its kinematic model and workspace are analyzed, the error analyses of the structure is presented with numerical simulations based on standard components used to construct it.

2. THE DIGITIZER DESCRIPTION

The developed digitizer is composed by a mechanical structure and a reading system. The reading system is made up by a laser beam source and a CCD (Charge-Coupled Device) as receiver, embedded in a compact unit. The reader system is based on the triangulation active spatial method to take the surface measures (Everett, 1995).

The mechanical structure of the digitizer has 5 dof and is composed of two kinematic chains, where one is used to move the laser sensor and the other one is used to take up the object. The structure which moves the laser sensor is composed of two revolute joints and one prismatic joint (a RRP structure), and the structure which takes up the object to pose it during the reading process is composed of a prismatic joint and a revolute ones where a table is assembled to support the object (a PR structure).

Using a RRP+PR structure can be justified because it respects the restrictions imposed by the triangulation method, it can be constructed in a robust way, presents good repeatability and the kinematical model can be obtained in a closed form which enable takes up the surface coordinates in function of the structure characteristics. In the Figure 1 an illustration of the developed digitizer is presented.

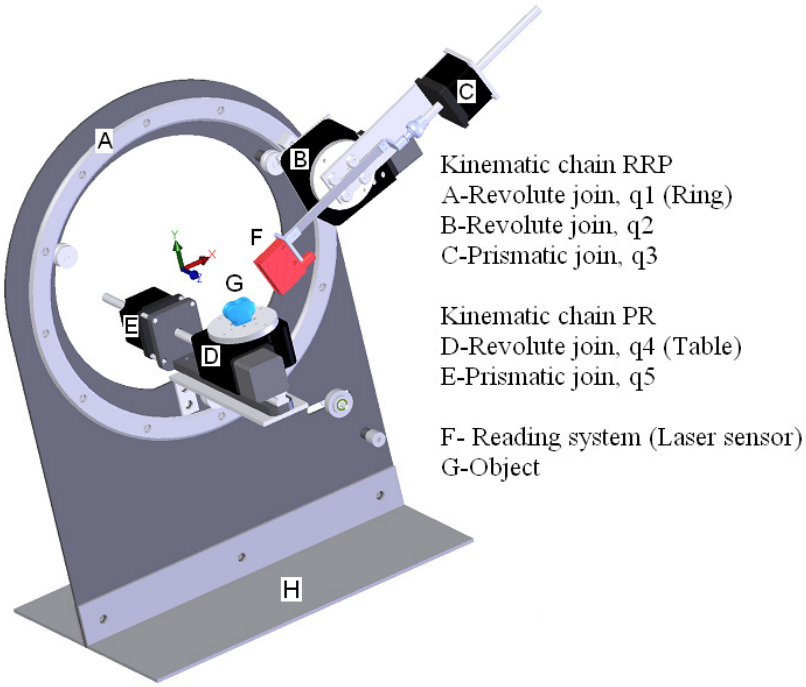

Figure 1. Mechanical structure of digitizer.

3. KINEMATIC MODEL

In order to obtain the kinematic model of the RRP+PR structure it must be considered that for any point Q of the surface its normal $\boldsymbol{N}$ must be oriented to the laser beam to enable the reading process. Then, in the system the Q point and its normal $\boldsymbol{N}$ must be put in the lecture plane defined by the laser beam. This re-positioning process is done by the PR structure.

In Figure 2 is represented the used inertial reference frame ($O_o\ X\ Y\ Z$), a generic Q point with its normal which its orientation is defined by angles η and γ, and auxiliary reference frames.

To pose the Q point and its normal in the XY-plane firstly the prismatic joint moves by q_5 and then the revolute joint turns by q_4. After the both motion the point Q is in the XY-plane with the denomination Q_1, as sketched in Fig. 3.

Using the classical homogeneous transformation matrix and equipollent reference frames, the homogeneous matrix between reference frames ($O_o\ X\ Y\ Z$) and ($O_5\ x_5\ y_5\ z_5$) can be given by

$$T_{05} = \left[\begin{array}{ccc|c} c(q_4+\gamma)\cdot c\eta & -c(q_4+\gamma)\cdot s\eta & s(q_4+\gamma) & x_Q\cdot cq_4 + z_Q\cdot sq_4 \\ s\eta & c\eta & 0 & y_Q \\ -s(q_4+\gamma)\cdot c\eta & s(q_4+\gamma)\cdot s\eta & c(q_4+\gamma) & -x_Q\cdot sq_4 + z_Q\cdot cq_4 + q_5 \\ \hline 0 & 0 & 0 & 1 \end{array}\right] \tag{1}$$

Where sq represents $sinq$ and cq is $cosq$.

By considering the new situation of the Q point in XY-plane, defined by point Q_1, and its normal as $\bar{N}$, the homogeneous matrix between reference frames ($O_o\ X\ Y\ Z$) and ($O_{5*}\ x_{5*}\ y_{5*}\ z_{5*}$), Fig.3, can be written as

$$T_{05^*} = \left[\begin{array}{ccc|c} c\eta & -s\eta & 0 & x_{Q_1} \\ s\eta & c\eta & 0 & y_{Q_1} \\ 0 & 0 & 1 & 0 \\ \hline 0 & 0 & 0 & 1 \end{array}\right] \tag{2}$$

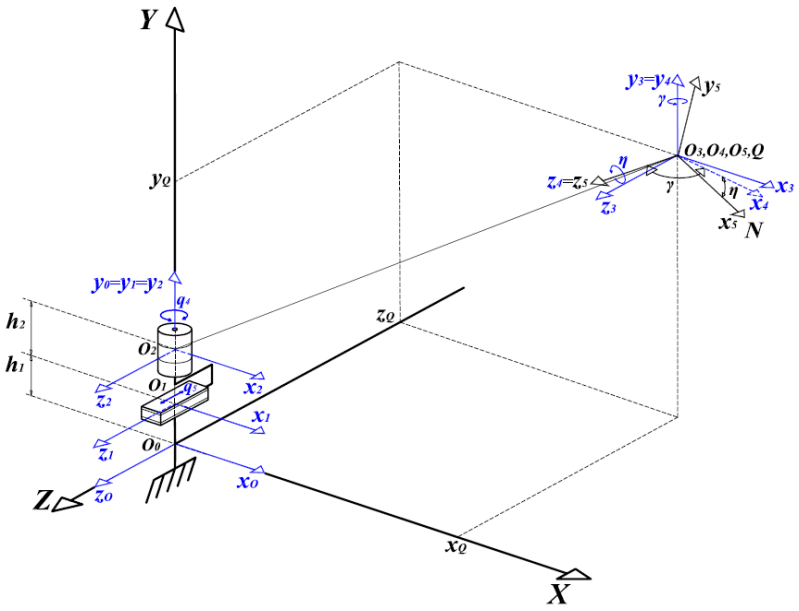

Figure 2. References frames for PR structure.

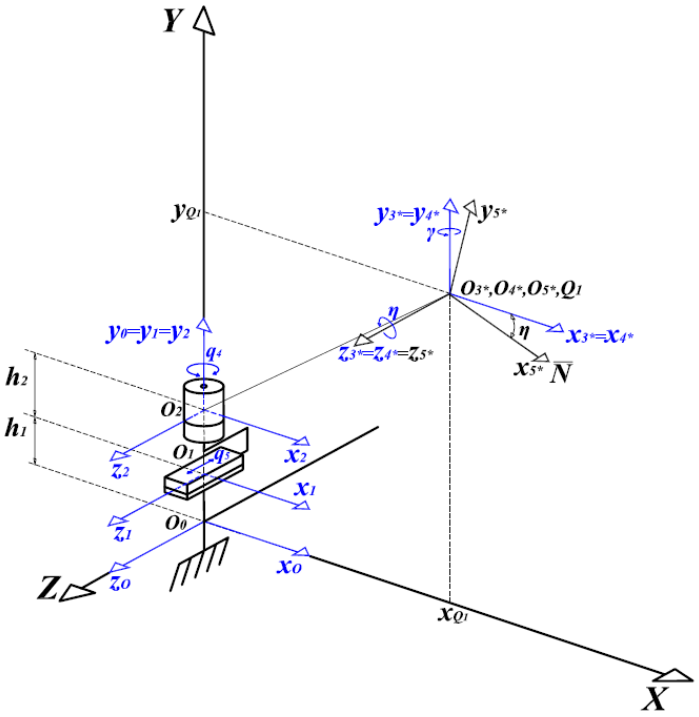

Figure 3. Reference frames for the new position of point Q in XY-plane, defined by Q_1 point.

From Equations (1) and (2) the coordinates of the new situation of the point Q in the XY-plane, defined by the point Q_1 can be given by

$$x_Q = x_{Q_1} \cdot cq_4 + q_5 \cdot sq_4 \tag{3}$$

$$y_Q = y_{Q_1} \tag{4}$$

$$z_Q = x_{Q_1} \cdot sq_4 - q_5 \cdot cq_4 \tag{5}$$

And the motions of the PR structure defined by the q_4 and q_5 joint coordinates can be written as

$$q_4 = \begin{cases} -\gamma & \left(-\dfrac{\pi}{2} < \gamma \le \dfrac{\pi}{2}\right) \\ \pi - \gamma & \left(\dfrac{\pi}{2} < \gamma \le 3 \cdot \dfrac{\pi}{2}\right) \end{cases} \tag{6}$$

$$q_5 = x_Q \cdot sq_4 - z_Q \cdot cq_4 \tag{7}$$

The kinematic analysis of the RRP structure can be done by considering it in an initial configuration as sketched in Fig. 4, where the Q_1 point and its normal $\bar{N}$ are represented too.

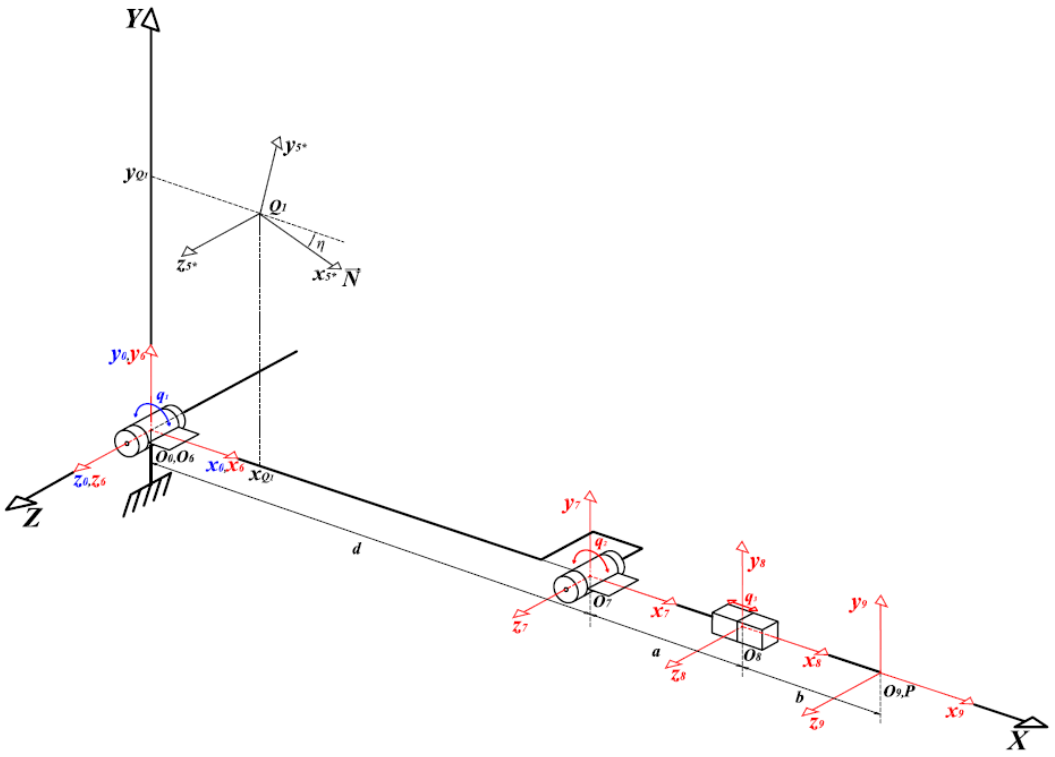

Figure 4. Reference frames of the RRP kinematic chain on its initial configuration.

In order to point out the laser beam to the normal direction the RRP configuration must be changed as sketched in Fig. 5, where the following structural parameters are used: d is the radius of the ring (the distance between the revolute joints); a is distance between the centers of the second revolute joint and the prismatic one at the initial configuration, and b corresponds to the length of the laser beam (given by the sensor), Fig. 4 and Fig. 5.

From Figures 4 and 5 and using the homogeneous matrices one can be write

$$T_{09} = \left[\begin{array}{ccc|c} c(q_1+q_2) & -s(q_1+q_2) & 0 & d \cdot cq_1 + (a+b+q_3) \cdot c(q_1+q_2) \\ s(q_1+q_2) & c(q_1+q_2) & 0 & d \cdot sq_1 + (a+b+q_3) \cdot s(q_1+q_2) \\ 0 & 0 & 1 & 0 \\ \hline 0 & 0 & 0 & 1 \end{array}\right] \tag{8}$$

$$T_{09*} = \left[\begin{array}{ccc|c} -c\eta & -s\eta & 0 & x_{Q_1} \\ s\eta & -c\eta & 0 & y_{Q_1} \\ 0 & 0 & 1 & z_{Q_1} \\ \hline 0 & 0 & 0 & 1 \end{array}\right] \tag{9}$$

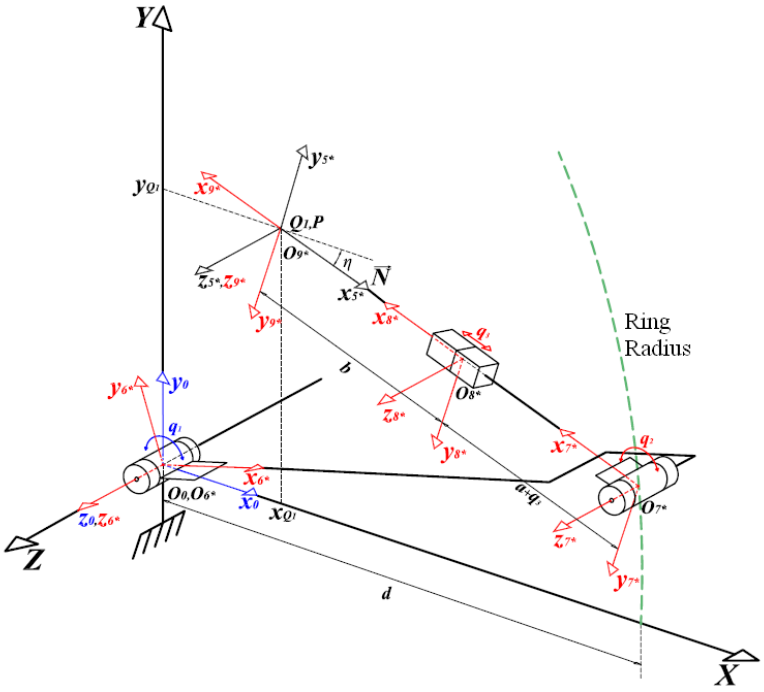

Figure 5. The RRP structure pointing up the laser beam to the normal $\bar{N}$ and the used reference frames

From Equations (8) and (9) the coordinates of point Q_1 can be obtained as

$$x_{Q_1} = d \cdot cq_1 + (a + b + q_3) \cdot c(q_1 + q_2) \tag{10}$$

$$y_{Q_1} = d \cdot sq_1 + (a + b + q_3) \cdot s(q_1 + q_2) \tag{11}$$

$$z_{Q_1} = 0 \tag{12}$$

and then, from Eqs. (3) to (12) one has

$$q_1 = arcsen\left[\frac{1}{d}\left(-x_{Q_1} \cdot s\eta + y_{Q_1} \cdot c\eta\right)\right] + \eta \tag{13}$$

$$q_2 = \pi + \eta - q_1 ; \left(-\frac{\pi}{2} < \eta \leq 3 \cdot \frac{\pi}{2}\right) \tag{14}$$

$$q_3 = -x_{Q_1} \cdot c\eta - y_{Q_1} \cdot s\eta - d \cdot cq_2 - a - b \tag{15}$$

Then, if the joint coordinates q_1, q_2, q_3, q_4 and q_5 are known, given by the digitizer system, the position of a point Q of the 3D surface and its normal direction, defined by angles η and γ can be obtained from Eqs. (3) to (15). The set of the Q coordinates will be used to reconstruct the object.

From the kinematics analysis of the RRP+PR structure its workspace can be obtained. Considering that the normal was put in the lecture plane (XY- plane) and using commercial components, where the ring radius is 175,5 mm, and considering the limits for the prismatic joint q_3 as $q_{3min}=0$ and q_{3max}=120 mm, the workspace of the RRP structure as a function of the normal orientation η can be obtained, as shown in Fig. 6. In this case, the η parameter is represented in

the interval $0 \leq \eta \leq \pi$ and $a+b$=57,5 mm. The workspace is the region comprised between the upper and the lower surface in Fig. 6.

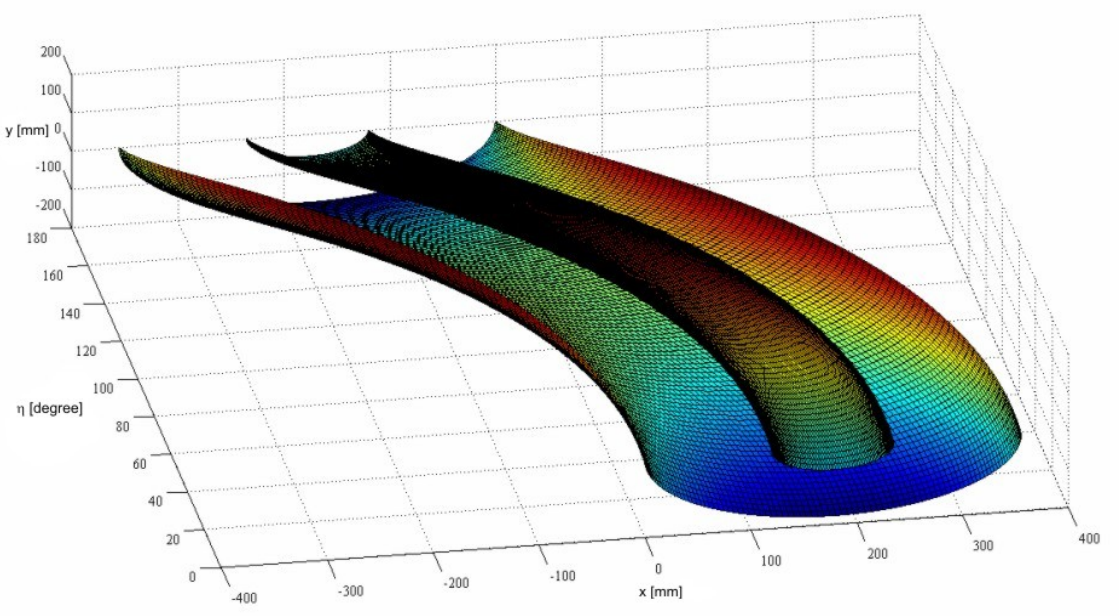

Figure 6. Workspace of the RRP structure in function of η.

4. ERROR ANALYSIS OF THE STRUCTURE

The characteristic parameters of the structure are submitted to errors affecting the final reading of the position of point Q and orientation of the vector $\boldsymbol{N}$. The errors are due to the reading system and the mechanical system. The errors from the reading system can be adjusted by a calibration that is made by programming. The errors due to the mechanical system are caused by the adjustments of the parts (geometric errors) and certains not geometric phenomena like as hysteresis, the joint friction and temperature; affecting with this the repetibilidade of the reached positions (Moring and Pack, 1986).

The accuracy of a structure is the total deviation of a pre-established situation, considered as the correct situation, and the reached situation (Dominique, 2006) and can be obtained by the Jacobian J of the structure by the expression

$$\delta X = J.\delta q \tag{16}$$

Where δX represents the deviation of the situation of the end-effector (on position and orientation) and δq the errors due to the joint coordinates of the structure.

Considering that the normal is placed in the lecture XY- plane, the errors of the RRP structure can be analyzed by using the equations of the kinematic model. Then, the deviation can be obtained by considering errors δq_1 , δq_2 and δq_3 in joint coordinates q_1, q_2 and q_3, respectively. The analysis of Eq. (16) shows that the errors can be obtained directly by the difference between the theoretical and the deviated situation as given by Eqs. (17), (18) and (19) (Moring and Pack, 1986), (Asada and Slotine, 1986).

$$\delta x = x_{Q_1'} - x_{Q_1} \tag{17}$$

$$\delta y = y_{Q_1'} - y_{Q_1} \tag{18}$$

$$\delta \eta = \eta' - \eta \tag{19}$$

Where δx and δy represent the deviations on the x and y coordinates and $\delta \eta$ in the orientation, x_{Q_1} and y_{Q_1} the theoretical coordinates of the Q_1 point and, $x_{Q_1'}$ and $y_{Q_1'}$ the coordinates of the deviated point Q_1', η the theoretical orientation and η' the deviated orientation.

From the kinematic model and Eq. (19) one can note that the deviation in the orientation is given by the sum of the errors from the revolute joints δq_1 and δq_2, and does not depend of errors in the prismatic joint δq_3. In this way the position errors of point Q_1 can be analyzed by Eqs. (17) and (18) as follows.

The theoretical position of the point Q_1 is given by Eqs. (10) and (11) as

$$x_{Q_1} = d \cdot cq_1 + (a+b+q_3) \cdot c(q_1+q_2) \tag{20}$$

$$y_{Q_1} = d \cdot sq_1 + (a+b+q_3) \cdot s(q_1+q_2) \tag{21}$$

Considering the errors δq_1, δq_2 and δq_3 in Eqs. (20) and (21), the deviated coordinates becomes:

$$x_{Q_1'} = d \cdot c(q_1+\delta q_1) + (a+b+q_3+\delta q_3) \cdot c(q_1+\delta q_1+q_2+\delta q_2) \tag{22}$$

$$y_{Q_1'} = d \cdot s(q_1+\delta q_1) + (a+b+q_3+\delta q_3) \cdot s(q_1+\delta q_1+q_2+\delta q_2) \tag{23}$$

And the total error for position is

$$e = \sqrt{\delta x^2 + \delta y^2} \tag{24}$$

In order to verify the behavior of each joint error one note e_i the total error due to only the *i-th* error joint. A sensibility index μ_i which represents the influence of a joint error δq_i in the end-effector situation can be defined too. Then, the following relation can be written

$$\mu_i = \frac{e_i}{\delta q_i} \quad i = 1,2,3 \tag{25}$$

Numerical simulations have been made by considering commercial components which will be used to construct a prototype. In Figure 7 are represented deviations on the laser beam and the read point when errors δq_1, δq_2 and δq_3 are considered in joint coordinates q_1, q_2 and q_3, respectively.

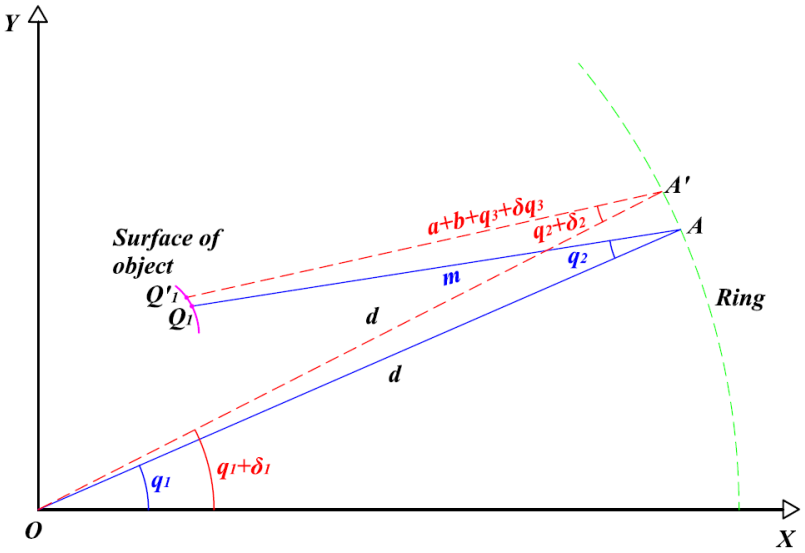

Figure 7. Sketch of the theoretical position of a point Q_1 and the real one Q'_1 by considering errors δq_1, δq_2 and δq_3 in joint coordinates q_1, q_2 and q_3, respectively.

As example, in Table 1 are presented simulation results for deviations in the position of a known point Q_1, given by its x_{Q1} and y_{Q1} coordinates, and the normal orientation η. In order to analyze the deviations it has been used for actuators of the revolute joints, q_1 and q_2, a resolution of 0,35 arc-seconds and repeatability of 5 arc-seconds, a resolution of 0,00635 mm for the actuator of the linear joint defined by q_3, and for the laser sensor a resolution of 0,1 mm. These

actuator characteristics enable to obtain the errors e_1, e_2 and e_3 in position of point Q_1 due to the errors in the q_1, q_2 and q_3 joint coordinates, respectively, and its correspondent sensibility index.

We can note that: the joint coordinate q_3 does not affect the normal direction, because the η angle does not depend on it, as commented before; from simulations it has been shown that the joint coordinate q_2 strongly affects the normal orientation, and both q_2 and q_3 joint coordinates must have excellent resolution in order to obtain all points of a 3D surface. The high values of μ_2 in Table 1 show the strong sensibility when errors exist in the q_2 joint coordinate. Satisfying these characteristics, the obtained cloud of points is uniform and without gaps well representing the 3D-surface of the object.

Table 1. Results of error analysis

η [°]	x_{Q1} [mm]	y_{Q1} [mm]	$x_{Q'}$ [mm]	$y_{Q'}$ [mm]	e_1[mm]	μ_1	e_2[mm]	μ_2	e_3[mm]	μ_3
163,1380	-17,8486	-2,1431	-17,8474	-2,1399	0,0004	17,9768	0,0039	158,8915	0,1064	1,0000
188,2021	-21,9436	-19,1299	-21,9437	-19,1268	0,0007	29,1115	0,0036	150,3386	0,1064	1,0000
76,5300	-7,6595	-29,2281	-7,6623	-29,2291	0,0007	30,2150	0,0036	148,2800	0,1064	1,0000
38,2582	6,2223	-17,5231	6,2203	-17,5260	0,0005	18,5951	0,0039	159,4838	0,1064	1,0000
-79,5429	18,2350	-13,3539	18,2018	-13,3542	0,0005	22,6018	0,0038	158,3717	0,1064	1,0000
-6,0891	32,4402	-1,1226	32,4399	-1,1253	0,0008	32,4597	0,0035	143,1083	0,1064	1,0000
75,0658	20,3964	12,8703	20,3998	12,8698	0,0006	24,1176	0,0038	157,0410	0,1064	1,0000
43,7973	7,1528	16,4398	7,1551	16,4371	0,0004	17,9284	0,0038	158,8227	0,1064	1,0000
67,4168	-5,3932	28,4863	-5,3905	28,4848	0,0007	28,9924	0,0036	150,5456	0,1064	1,0000
162,5900	-21,4196	21,4534	-21,4191	21,4563	0,0007	30,3158	0,0036	148,0784	0,1064	1,0000
202,0650	-18,3385	3,5018	-18,3400	3,5050	0,0005	18,6698	0,0039	159,5273	0,1064	1,0000

5. CONCLUSIONS

In this paper a RRP+PR structure had been described to use as digitizer of 3D-surfaces.

From its kinematic model, both the analysis of its workspace and the influence of the joint error in the position and the normal orientation, can be concluded that the actuators must have excellent resolution, principally the second revolute joint and the prismatic one of the RRP structure, in order to obtain all points of a 3D-surface.

Finally, a prototype is in construction based on the obtained results to read 3D-surfaces in association with a methodology for acquiring and processing the data of the surface.

5. ACKNOWLEDGEMENTS

The authors are thankful to CAPES, CNPq and FAPEMIG-Fundação de Amparo e Pesquisa do Estado de Minas Gerais for financing support of this research work from Project TEC 2166/07.

6. REFERENCES

Asada, H., Slotine, J.J.E., 1986, "Robot Analysis and Control". John Wiley & Sons, pp 51-71

Bajaj, C.L., Bernardini, F. and XU, G., 1995, "Automatic Reconstruction of Surfaces and Scalar Fields from 3D Scans". International Conference on Computer Graphics and Interactive Techniques Proceedings of the 22nd annual Conference on Computer Graphics and Interactive Techniques, pp. 109-118.

Dalton, G., 1998, "Reverse Engineering Using Laser Metrology". Sensor Review n. 18, v.2, pp. 92–96.

Dominique, P.D., 2006, "Contribution à la Modélisation et à l'Étalonnage Elasto-Géométriques des Manipulateurs à Structure Parallèle". PhD Thesis, Institut National des Sciences Appliquées de Rennes, France, pp.13-55.

Everett, H.R., 1995, "Sensors for Mobile Robots: Theory and Application". A K Peters, Wellesley, MA., c. 4, pp. 114-119.

Feng, H., Liu, Y., Xi, F., 2001, "Analysis of Digitizing Errors of a Laser Scanning System". Precision Engineering. n. 25, pp. 185–191.

Larsson, S. and Kjellander, J.A.P., 2006, "A Laser Profile Scanner and a Robot as Platform for Unattended Acquisition of Unknown 3D Objects". Örebro University, School of Science and Technology, pp. 1-13.

Larsson, S., Kjellander, J. A. P., 2008, "Path Planning for Laser Scanning with an Industrial Robot". Robotics and Autonomous Systems, n. 56, pp. 615–624.

Levoy, M., Curless, B., Pulli, K., Ginsberg, J., Ginzton, M., Koller, D., Pereira, L., Rusinkiewicz, S., 1998, "The Stanford Large Statue Scanner". Stanford University.

Li, J., Guo, Y., Zhu, J., Lin, X., Xin, Y., Duan, K., Tang, Q., 2007, “Large Depth-of-View Portable Three-Dimensional Laser Scanner and its Segmental Calibration for Robot Vision”. Optics and Lasers in Engineering, v. 45, pp. 1077–1087.

Milroy, M.J., Weir D.J., Bradley, C., Vickers, G.W., 1996, “Reverse Engineering Employing a 3D Laser Scanner: A Case Study”. International Journal of Advanced Manufacturing Technology. n.12, pp. 111–21.

Moccozet, L., Dellas, F., Magnenat-Thalmann, N., Biasotti, S., Mortara, M. and Falcidieno, B., 2004, “Animatable Human Body Model Reconstruction from 3D Scan Data Using Templates”. Proc. CapTech Workshop on Modelling and Motion Capture Techniques for Virtual Environments, Zermatt, Switzerland, pp. 73-79.

Mooring, B. and Pack, T., 1986, "Determination and Specification of Robot Repeatability". IEEE International Conference on Robotics and Automation, San Francisco, USA, pp. 1017-1023.

Müller, H.A., Jahnke, J.H., Smith, D.B., Storey, M., Tilley, S.R. and Wong, K., 2000, “Reverse Engineering: A Roadmap”. Proceedings of the Conference on the Future of Software Engineering, pp. 47-60

Remondino, F., 2003, “From Point Cloud to Surface: The Modeling and Visualization Problem”. The International Workshop on Visualization and Animation of Reality-based 3D-models, Tarasp-Vulpera, Switzerland, Vol. XXXIV-5/W10.

Várady, T., Martin, R. and Cox, J., 1997, “Reverse Engineering of Geometric Models–an Introduction”. Computer-Aided Design, n. 29, v. 44, Elsevier Science, pp. 255-268.

7. RESPONSIBILITY NOTICE

The authors are the only responsible for the printed material included in this paper.